COHERENT SYNCHROTRON RADIATION AND BUNCH COMPRESSION STUDIES IN THE EMITTANCE EXCHANGE BEAMLINE AT THE FERMILAB A0 PHOTOINJECTOR

J. C. T. Thangaraj *, R. Thurman-Keup, A. Johnson, J. Ruan, P. Piot,
M. Church, H. Edwards, A. Lumpkin, Y.-E Sun, T. Maxwell, J. Santucci, Fermilab, IL, USA

Abstract

One of the goals of the Fermilab A0 photoinjector is to investigate experimentally the transverse to longitudinal emittance exchange principle. Coherent synchrotron radiation in the emittance exchange line could limit the performance of the emittance exchanger at short bunch length. In this paper, we present experimental and simulation studies of the coherent synchroton radiation (CSR) in the emittance exchange line at A0 photoinjector. We also show how EEX can be used to compress a bunch by adding chirp to the incoming beam.

INTRODUCTION

Incoherent synchrotron radiation (ISR) is emitted when an electron bunch goes through a dipole bending magnet. When the wavelength of the synchrotron radiation is comparable to the bunchlength, then the radiation becomes coherent and is called coherent synchrotron radiation (CSR). The intensity of CSR goes as N^2, where N is the number of electrons in the bunch. Typically, an electron bunch contains 10^9 particles, causing this radiation to be orders of magnitude brighter than ISR. CSR causes at least two effects on the bunch. The first effect is the bunch loses energy due to CSR leading to an energy spread along the bunch. The power loss due to CSR can be expressed as: $P = \frac{N^2 x e^2}{\epsilon_0 \rho^{2/3} \sigma_z^{4/3}}$, where N is the number of particles, x is 0.0279, ρ is the bending radius , σ_z is the bunch length, and e is the charge of electron. Therefore, the shorter the bunch at the dipole, the larger the power loss due to CSR. Secondly, when the energy loss happens inside a bend, the energy spread is then converted to transverse projected emittance growth when the bunch exits the bend.

The emittance exchange principle, where the transverse and longitudinal emittance of the electron beam is exchanged, was originally proposed as a cure for the microbunching instability [1]. A proof-of-principle emittance exchange experiment (EEX) was built and demonstrated at the Fermilab A0 photoinjector [2]. There are also other applications for the emittance exchange beamline. For example, by adding a transverse mask to the incoming beam, 100-femtosecond bunches were generated using the emittance exchange principle [3].

The emittance exchange line (EEX) consists of a TM_{110} RF cavity sandwiched by two doglegs. The scheme is based on a variation of the original configuration proposed by Cornacchia, where the cavity was at the center of a chicane. A crucial advantage of the new scheme is the output emittances are uncoupled after the exchange [4]. However, the finite length of the cavity, space charge effects, coherent synchrotron radiation (CSR), and wakefields could lead to an imperfect emittance exchange.

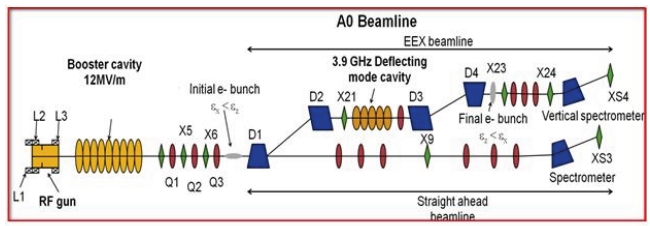

Figure 1: Experimental Setup of the A0 photoinjector facility. The quad before the dipole D3 is a skew quad.

In this work, we present experimental results from measuring CSR in the EEX beamline and its effect on the electron beam. We begin with a brief description of the experimental setup. Then, we present power, polarization and angular distribution measurements of the CSR from the third dipole. Finally, we report our results on bunch compression by operating the EEX beamline with an RF chirp.

EXPERIMENTAL SETUP

The A0 photoinjector facility (A0PI) consists of an L-band RF gun followed by a superconducting 9-cell booster cavity, which accelerates the e-beam up to 16 MeV. After acceleration, the beam is steered and focused using the dipoles and the quads (Q1 Q2 Q3). The beam then can either continue straight to XS3 or could be steered into the dogleg. In our experiments, the beam is sent through the doglegs (D1, D2, D3, D4) to the spectrometer (XS4). Between the doglegs is the 3.9 GHz deflecting mode cavity, which was switched on/off in our study. The experimental setup is shown in Figure 1. When the bunch passes through the dogleg, CSR is expected to be more pronounced at dipole 3. So, we installed optics to collect the radiation coming out of the port at D3. The light is collimated using an off-axis parabolic mirror onto a plane mirror. The reflected light is then directed to a pyroelectric detector for power measurement [5]. Bunch length measurements reported in this work uses the coherent transition radiation light from X24.

* jtobin@fnal.gov

ISBN 978-3-95450-117-5

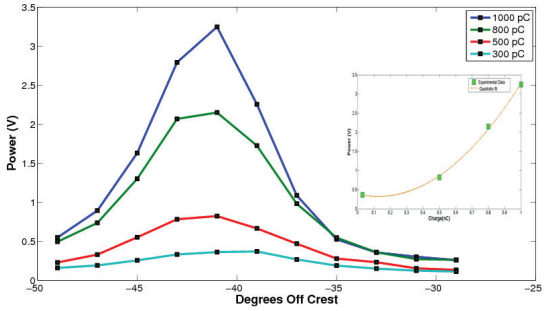

Figure 2: CSR Power measurement at dipole 3 as a function of 9-cell booster cavity phase. Maximum power is observed at 41 degrees off crest. The number of bunches was 10. Increasing the number of bunches saturated the pyroelectric detector. The inset shows the power as a function of charge with a quadractic fit.

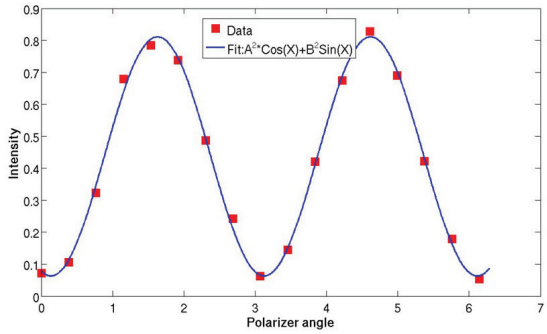

Figure 3: The measured CSR intensity as a function of polarizer angle. The baseline is not zero indicating the vertical polarization component of the CSR light.

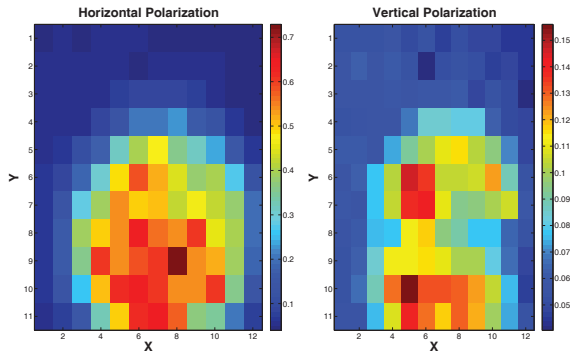

Figure 4: Measured angular distribution of the CSR radiation with horizontal polarization (left) and with vertical polarization (right). The ratio between the maximum value of the horizontal to the vertical is 4.6. The scanned window area is 55x60 mm^2. The vertical polarization shows the expected dip at the center.

EXPERIMENTAL RESULTS

CSR Power Measurements

Synchrotron radiation is predominantly horizontally polarized. When the condition for coherency is satisfied, the single particle radiation intensity is multiplied by the bunch form factor and N^2. We measured the intensity of the radiation for various bunch charges and at different RF phases. We found that the detector power is maximum at the minimum bunchlength for a fixed charge as expected from the calculation [5]. Moreover, the detected power also varies quadratically with charge as expected from coherent radiation. This is shown in Figure 2. Comparison between charges with a fixed number of bunches in a bunch train poses a limitation because the pyrometer gets saturated for higher charge at a lower number of bunches. The number of bunches we chose was 10 to prevent the pyrometer from saturating at 1nC.

Polarization and Angular Distribution

A wire-grid polarizer, which could be remotely rotated, was installed in front of the pyrodetector. The grids consist of 15 μm diameter gold-plated tungsten wires spaced by 45 μm.The intensity of the CSR was measured as a function of the polarizer angle. This is shown in Figure 3 along with a fit function. As expected, the light is mostly horizontally polarized. Assuming an electric field $\overrightarrow{E_x}$ and $\overrightarrow{E_y}$ for the horizontal and the vertical polarization components, incident at an angle of θ at the polarizer, the electric field after the polarizer is given by $\overrightarrow{E_t} = \overrightarrow{E_x}\cos\theta + j\overrightarrow{E_y}sin\theta$. So, the intensity at the detector is $|E_t|^2 = \overrightarrow{E_t}.\overrightarrow{E_t^*} = E_x^2\cos^2\theta + E_y^2\sin^2\theta$.

To map the angular distribution of the light, the detector was mounted on an X-Y translation stage and scanned over an area of 55 mm x 60 mm with 5 mm step size on each direction. The measurement was done for both horizontal and vertical polarizations. This is shown in Figure 4. The measured ratio between the horizontal and the vertical polarization was 4.6. Theoretically, the horizontal polarization carries 7 times more power than the vertical. The discrepancy may be due to several factors: the theory assumes collection of all frequencies over all angles, while in the experiment, we are limited by the finite geometry of the beam pipe cutting off some frequencies and the diffraction limitation of the relay optics.

Skew Quad

In order to study the effect of CSR on the beam, a skew quad was installed before the dipole D3. At the skew quad, the particle receives a y kick proportional to its x-position, $y' = \frac{x}{F}$ where F is the focal length of the skew quad. This kick is converted to a y-position change at the screen: $y_{screen} = R_{34}y'_{quad}$. In terms of r.m.s. quantities, as long as the β_y at the screen is small, the y-beamsize is, $\sigma_{y_{screen}} = \frac{\sigma_{x_{quad}}}{K}$ where K is a constant and $\sigma_{xquad} = \sqrt{x_\beta + (\eta\delta)^2}$ where η is the dispersion and δ

ISBN 978-3-95450-117-5

is the energy spread and x_{beta} is the beamsize due to the betafunction and emittance. If the beam size at the skew quad is dominated by dispersion (like in a bunch compressor) and assuming a linear chirp ($\delta = hz_{in}$), we can write: $\sigma_{y_{screen}} = \frac{hz_{in}}{K}$. After cancelling dispersion, the y-beamsize is proportional to incoming bunchlength. In our setup, the dispersion is cancelled by using the last three quads downstream of the X23 screen station.

Twin Pulse Transport

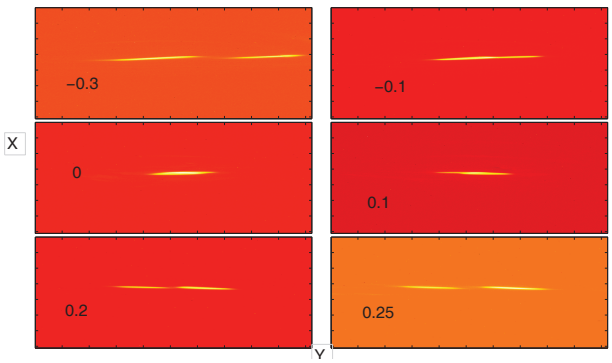

Figure 5: Experiment: Twin pulses observed at X24. The bottom left value in each plot is the skew quad current in Amps. When the skew quad is off, no pulse separation is observed. When the skew quad is turned on, the separation in the pulses is observed. The 5-cell was turned off.

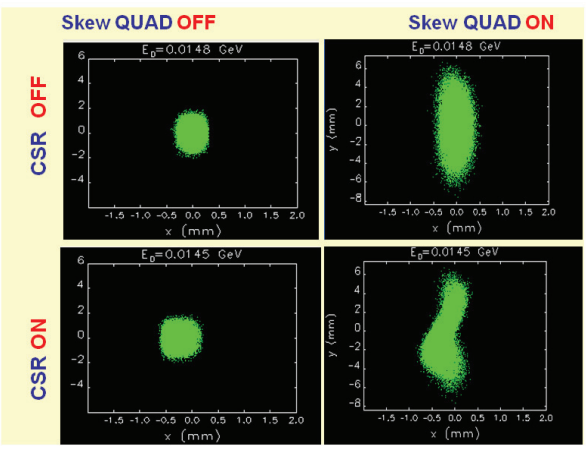

Figure 6: Simulation: *elegant* showing the effect of CSR and skew quad at X24. Due to CSR, the head particles get higher energy leading to a transverse offset. The 5-cell was switched off.

To begin our study, we used two laser pulses separated in time and then turned on the skew quad to see if the time separation is revealed on the screen. The electron pulses separated in time experience different accelerating field in the 9-cell and end up with different energies, but this does not show a position change at X24 because the dispersion is cancelled at X24 using the quads. By turning on the skew quad dispersion leaks to the y-plane - thereby acting like a vertical deflector. This is shown in Figure 5. Thus the skew quad can be used to time resolve the x-beamsize at X24.

We used *BeamLattice* [6] and *elegant* [7] programs to study the effect of skew quad on beam dynamics. After optimizing the betafunction using *elegant*, we turned on CSR effects in *elegant* by introducing CSRSCBEND and CSRDRIFT elements. The results, when the deflecting cavity is off, are shown in Figure 6. CSR modulates the energy by accelerating the head which results in a change in the transverse positions of the particles as they exit the bend. Here we have made a thin-lens approximation for the 5-cell and have ignored other collective effects like space charge and wakefields. The case with 5-cell on is investigated in [8]. The measured image profile at X24 for various charges with and without the skew quad on is shown in the Figure 7. As the charge increases, the CSR "bulge" effect is seen on the screen in the two lower column on the right hand column in Figure 7. This is consistent with the CSR power measurement in Figure 2, where increase in charge shows a quadratic increase in CSR power loss indicating that the CSR effect is more pronounced at higher charges.

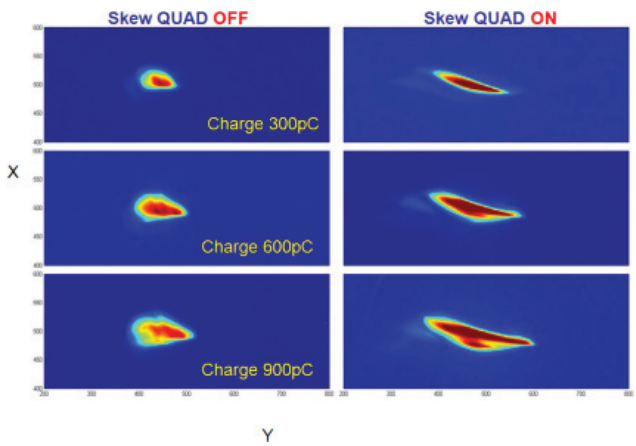

Figure 7: Measured transverse beam profile as a function of skew quad for various charges.No skew quad (left) and with skew quad(right). The CSR bulge effect is prominent at higher charges. The image is rotated by 90^0 compared to Figure 6. When the skew quad is turned on, the y-axis on the right is proportional to the incoming bunchlength.

BUNCH COMPRESSION

In the emittance exchange beamline, if we assume a thick lens for the cavity, the transfer matrix is altered with coupling from incoming z and δ [2]. So, the outgoing paricle $z_2 = \kappa\xi x_1 + \left[\frac{-1}{\kappa} + \left(\frac{L_c}{4} + L\right)\xi\right]\kappa x_1' + \frac{L_c\kappa^2\xi}{4}(z_1 + \xi\delta_1)$ where ξ is the longitudinal dispersion, x_1, x_1', z, δ are the incoming x, x', longitudinal position, energy spread of the beam and L_c, L, κ are the length of the cavity, the length of the dogleg and the strength of the

ISBN 978-3-95450-117-5

cavity respectively. If we set $chirp = \frac{\delta_1}{z_1} = \frac{-1}{\xi}$, then the last term in the equation will be minimized.

During the emittance exchange experiment, the beam injected into the EEX beamline has no chirp. We imparted a chirp on the beam by operating the 9-cell off-crest and the bunchlength of the electron beam at X24 was measured with a streak camera. For Q1AX03 between 0.35 to 0.55, the bunchlength reached the resolution limit of the streak camera (∼300 fs). We then did power measurements with both the bolometer and pyro-detector for a beam with and without chirp. This showed a factor of 2 increase in power detected for the beam with chirp. This motivated us to operate the EEX beamline with a chirp for the beam and to use the Martin-Puplett interferometer for the bunchlength measurement. The CTR radiation from X24 was used to measure the auto-correlation of the beam with and without energy chirp. The result is shown in Figure 8.

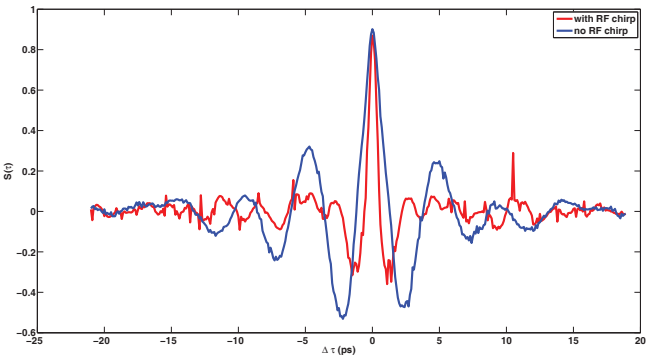

Figure 8: Auto-correlation measurement with Martin-Puplett interferometer with and without energy chirp. The beam with an RF chirp is shorter compared to the one without chirp.

The bunch with chirp (red) shows a shorter auto-correlation width compared with the bunch with no chirp (blue). Assuming a Gaussian bunch and extracting the bunchlength from the auto-correlation using the formula: $\sigma_t = \frac{FWHM_{center}}{2.35\sqrt{(2)}}$ where $FWHM_{center}$ corresponds to the full-width half maximum of the center peak, yields a bunchlength of 0.60 ps (blue) and 0.25 ps (red). Therefore, adding a chirp decreases the bunchlength by a factor of ∼2.4. This in agreement with the power measurements which also show a factor of ∼2 increase in the detector power for a beam with chirp and also agrees with the theoretical predictions and computer simulations. The bunchlength formula has been verified through computer simulation which assumes a Gaussian bunch along with a diamond window for the extraction port.

In the experiment, the bunch is not Gaussian and the detector response is not uniform at these frequencies as well. Further data is being investigated to get an accurate measurement of the bunch profile and bunch length. Electro-optic sampling is being developed as an alternative diagnostic at A0 photoinjector, which could possibly reveal the bunch profile [9].

CONCLUSION AND FUTURE WORK

In this work, we have reported on CSR power, polarization and angular distribution measurements. We have also reported on the ability of the skew quad to time-resolve the beam size at X24. Finally, we have shown that imparting an energy chirp on the beam leads to a shorter bunch after the EEX beam line. To accurately measure the bunchlength, electro-optic sampling is being pursued.

ACKNOWLEDGMENTS

This work was supported by the U.S. Department of Energy . The experiment is funded by Fermi Research Alliance, LLC under Contract No. DE-AC02-07CH11359 with the U.S. Department of Energy.

REFERENCES

[1] M. Cornacchia and P. Emma, Physical Review Special Topics - Accelerators and Beams 5 (8), 084001 (2002).

[2] J. Ruan et. al, "First Observation of the Exchange of Transverse and Longitudinal Emittances", Phys. Rev. Lett. 24 (2011) 106

[3] Y. E-Sun et. al, "Tunable Subpicosecond Electron-Bunch-Train Generation Using a Transverse-To-Longitudinal Phase-Space Exchange Technique", Phys. Rev. Lett. 23 (2010)105

[4] A. Johnson et. al, "Demonstration of Transverse-to-Longitudinal Emittance Exchange at the Fermilab Photoinjector", IPAC 2010, Kyoto, Japan, 2010, THPE043

[5] J. C. T. Thangaraj et. al, "Experimental Study of Coherent Synchrotron Radiation in the Emittance Exchange Line at the A0-Photoinjector", AAC 2010, Annapolis, 2010, AIP Conference Proceedings, p. 643-646.

[6] An inhouse MATLAB code based on TRACE3D developed by R.Thurman-Keup

[7] M. Borland, "elegant: A Flexible SDDS-compliant Code for Accelerator Simulation", Advanced Photon Source LS-287, September 2000

[8] J. C. T. Thangaraj et. al, "Experimental Study of Coherent Synchrotron Radiation in the Emittance Exchange Line at the A0-Photoinjector", PAC Proceedings 2011, New York, 2011

[9] T. Maxwell and P. Piot, "Proposal for a non-interceptive spatio-temporal correlation monitor", PAC Proceedings 2009, Vancouver, 2009

ISBN 978-3-95450-117-5